RSC Advances




ROYAL SOCIETY OF CHEMISTRY

www.rsc.org/advances

# One-Pot Synthesis of Chitosan- Dehydropregnanolone Acetate Ketimine Nanoparticles and Antifungal Bioevaluation

**Archana M. Das [1]*, Raju Khan [2], Manash P. Hazarika [1], Debjani Baruah[1], Purnajyoti D Bhuyan [3]**

**[1]Natural Products Chemistry Division, [2]Analytical Chemistry Division, [3]Medicinal and Aromatic Plant Division**

CSIR-North East Institute of Science & Technology

Jorhat – 785 006, Assam, India.

## ABSTRACT

This paper presents a new method for fabrication of biodegradable bio-polymeric nanoparticles, via convenient one-pot strategy at room temperature in stirring condition for application of communicable diseases. The simultaneous synthesis and assembly of chitosan-16-dehydropregnanolone acetate (CHDPA) nanoparticles were characterized by Fourier transform infrared (FT-IR) spectra, $^{1}$H NMR and UV vis analysis and morphology along-with particle size were identified by scanning electron microscopy (SEM) and transmission electron microscopy (TEM). In this study, the antifungal property of the CHDPA nanoparticle was exploited for antifungal activity against the fungus *Colletotrichum gleosporioides.* The drug loading capacity (LC), encapsulation efficiency (EE) and drug release study were investigated using UV spectrophotometer.

**KEY WORDS** : Chitosan; 16-dehydropregnenolone acetate; Nanoparticles; biodegradable; antifungal activity; *Colletotrichum gleosporioides*.

---

*Corresponding author:

Email : archanads2@gmail.com

Phone: +919435489369

## Introduction

Nanostructured materials have much attention role in many biology related applications and advanced nanodevices in recent day scenario of bio-nanotechnology. The assembly of nanostructures across several length-scales is also of paramount importance in the synthesis of organized materials with advanced functions. Chitosan, a natural based-polymer obtained by alkaline deacetylation of chitin, is nontoxic, biocompatible, and biodegradable. Owing to its properties, chitosan can be used in medicine, pharmacy, biotechnology, agriculture, biodegradability, biocompatibility, and antimicrobial activity and the food industry[1-4]. The polycationic biopolymer is receiving a great deal of attention for biosensing, medical, and pharmaceutical applications [5-7] and it is the most commonly used natural polymer in regenerative medicine and tissue engineering [8]. Chitosan micro- or nanofibers have been widely accepted as biomedical scaffolding materials to restore, maintain, or improve the functions of various tissues [9-10]. Therefore, the creation of chitosan nanostructures with controllable morphology is highly desirable, but has met with limited success yet. However, one elegant method, electrospinning, has been reported for producing chitosan nanofibers. Because of their biocompatibility and biodegradability, the resulting chitosan nanostructures can be potentially tailored to mimic a natural extracellular matrix, to achieve controlled drug delivery, and to develop tissue-compatible scaffolds for tissue cultures. Thus, derived chitosan possesses many useful biological properties such as biocompatibility, biodegradation, woundhealing and anti-bacterial action [1, 11-13]. Therefore, much attention has been paid to develop chitosan-based biomedical materials. Chemical modification of

chitosan is useful for the association of bioactive molecules to polymer and controlling the drug release profile.

In this study, the nanostructure mechanical property, and biocompatibility of the novel chitosan/16-DPA particles were evaluated. It has been widely used in pharmaceutical research and in industry as a carrier for drug delivery and as biomedical material [14]. Chitosan was selected for nanoparticles because of its recognized mucoadhesivity and ability to enhance the penetration of large molecules across mucosal surface [15].

Our effort has been concentrated to synthesized hybrid nanoparticles using a convenient one-pot method and by literature survey no work has been reported, particularly 16-Dehydropregnenolone Acetate. Significantly, our results show that a polymer of single composition and short length could contribute to the growth of highly anisotropic structures. Such an anisotropic aggregation is most likely due to the nonuniform distribution of capping agents on the steroid nanoparticle amorphous surfaces. The aim of the present investigation has been describe the synthesis and characterization of novel biodegradable nanoparticles based on chitosan for encapsulation of 16-DPA and the product has screened for antifungal activity against the fungus *Colletotrichum gleosporioides.* The drug loading capacity (LC), encapsulation efficiency (EE) and drug release study were investigated using UV spectrophotometer.

## 2. Materials and methods

### *2.1. Materials and chemicals*

Chitosan (CH) (MW 2.4 x$10^6$), 16-dehydropregnanolone acetate (16-DPA), N, N-dicyclo-hexyl carbodiimide (DCC) and 4-dimethyl amino pyridine (DMAP) were purchased from Sigma-Aldrich and used directly without purification. Acetonitrile, ethyl acetate, methanol, NaCl, $Na_2HPO_4$ and $KH_2PO_4$ were purchased from CDH analytical

grade and only distilled solvents were used for the reactions. Triple distilled $H_20$ was used for preparation of the solutions.

*2.2. Methodology*

*2.2.1. Synthesis of Chitosan-16-DPA nanoparticles*

A solution of 16-DPA (100 mg) in MeOH (60 ml) was stirred for 10 min. at room temperature and 25 ml of 1% chitosan solution was added slowly. A solution of DCC (100 mg) in MeOH (5 ml) was added and after that DMAP (300 mg) in MeOH (5 ml) was added to catalyze the reaction system [16]. The reaction mixture was stirred for 24 hrs at room temperature. In order to enhance the precipitation of the by-products the resulting suspension was treated with acetonitrile (30 ml). The resulting solution was filtered and the filtrate was evaporated under reduced pressure to get the product. After that the product was redissolved in ethyl acetate (50 ml) and discard the undissolved by-products by filtration. Ethyl acetate was evaporated under reduced pressure to get the final required product. Purified the product by washing with MeOH and finally white crystalline solid products was formed.

*2.2.2. General Methods*

Melting points were measured with a Buchi B-540 melting point apparatus and are uncorrected. The progress of each of the reaction was monitored on Merck thin layer chromatography silica gel 60 F254. IR spectra were recorded with a Perkin-Elmer model 2000 series FT-IR spectrometer for solutions in chloroform. Infrared absorbance is reported in reciprocal centimeters ($cm^{-1}$). $^{1}H$ and $^{13}C$ NMR spectra were recorded on a Bruker DPX (300 MHz) spectrometer using $CDCl_3$ or DMSO-$d_6$ as solvent with tetramethylsilane (TMS) as internal standard on ppm scale (δ). Multiplicity of the

resonance peaks are indicated as singlet (s), broad singlet (bs), doublet (d), triplet (t), quartet (q) and multiplet (m). The surface morphologies were examined by using a Scanning Electron Microscopy (SEM; JSM-35, JEOL, Japan). The particles were made conductive by sputter-coating with palladium prior to SEM analysis. The particle size of the polymeric aggregates was observed using a TEM (JEM-2000 FX II, JEOL, Japan). A drop of the product suspension was placed on a copper grid coated with carbon film, dried at 25 $^{0}$C and observation was performed at 80 kV.

2.2.3. *In vitro* antifungal activity

2.2.3.1. Fungus and media

The antifungal activity of the new modified chitosan (CHDPA) was studied against the fungus *Colletotrichum gleosporioides.*

The inhibitory effects of the samples were tested in vitro on mycelia growth of *Alternaria alternata*. Poisoned Food technique[17-18] was used to test the antifungal activity of the sample. Samples were used at concentrations of 100, 200, 300, 400 and 500 ppm. Petriplates (90 mm dia.) each containing 20 ml of potato dextrose agar (PDA) medium amended with the desired concentrations of samples were inoculated with test fungus. A 5 mm diameter disc of the test fungus with a corkborer, cut from the periphery of an actively growing 8 -days old culture on PDA plates and was placed at the center in each treated petriplate PDA plates without sample served as control, which consist of 100, 200, 300, 400 and 500 ppm of the solvent. The experiments were conducted with three replications. Then plates were kept in incubator at temp. 25 ±1°C. Fungal growth was observed at every 24 hrs. interval. At the end of the incubation period, after 72 hrs. the minimum inhibitory concentration (MIC) that caused complete inhibition of the mycelia

126 growth was measured. The percentage of inhibition of mycelial growth was calculated
127 from mean values of colony diameter in treated and control petridishes using the
128 following formula [18].

129 Inhibition % = 100 (Control-Treatment) / Control

130 *2.2.4. Phosphate Buffer Saline pH 7.4*

131 Phosphate buffered saline is a buffer solution commonly used in biological research[19].
132 1 liter stock of 10x PBS was prepared by dissolving 8 g NaCl, 1.44 g $Na_2HPO_4$ and 0.24
133 g $KH_2PO_4$ in 800 ml of distilled water, and topping up to 1 Lit. The pH is ~6.8, but when
134 diluted to 1x PBS it should change to 7.4.

135 *2.2.5. Standard graph for Drug content*
136
137 Stock solution was prepared[19] by dissolving DPA (10 mg) in suitable solvent or
138 buffer (1ml solvent+9 ml buffer) and 1 ml of mixture from the stock solution was diluted
139 with 9 ml of phosphate buffer saline pH 7.4 which is used as a standard solution. Aliquots
140 of standard solution were further diluted with phosphate buffer saline pH 7.4 to get
141 working solution of 5, 10, 15, 20 and 25 µg/ml. The working standards were scanned
142 using UV spectrophotometer which shows the maximum absorbance at lambda max. The
143 same λ max was used for the further measurement of the drug. Finally, the prepared
144 standards were measured, in each case against a solvent blank similarly prepared and
145 calibration the graphs of the absorbance *versus* the concentration of the drug was plotted.

146 *2.2.6. Determination of DPA Loading Capacity (LC) & Encapsulation Efficiency (EE)*
147
148 Proper amounts of product were mechanically ground in a mortar with a pestle.
149 About 5 mg of the product were placed into a 10 ml standard flask with a cap and add 10
150 ml of suitable solvent. After the mixture in the flask was broken up by ultrasonication for

30 min, the flask was capped and shaked for 24 h at room temperature. Finally, the mixture was transferred into a 25 mL flask and diluted to 25 mL with solvent. The suspension was filtered through a 0.45 μm membrane. The concentration of drug in the filtered solution was measured at wavelength of lamda max[19].

The recovery of the product (final product amount) was defined as the weight ratio of dried product to the initial loadings of polymer and drug. The dried product was dissolved in acetonitrile, sonicated for 5min and then distilled water was added to precipitate the polymer preferentially. The drug content in the supernatant after centrifugation (15,000 for 15min) was measured spectrophotometrically at particular lambda max for each drug by Ultra Violet spectroscopy (UV). The product recovery, drug loading capacity and encapsulation in the product were calculated using the following equations[19].

$$\text{Percentage of Nanoparticle Recovery} = \frac{\text{Mass of nanoparticles recovered}}{\text{Mass of drug}} \text{ X } 100$$

$$\text{Percentage of Drug Loading Capacity (W/W)} = \frac{\text{Mass of DPA in nanoparticles}}{\text{Mass of product recovered}} \text{ X } 100$$

$$\text{Percentage of Drug Encapsulation} = \frac{\text{Mass of drug in nanoparticles}}{\text{Mass of drug used in the formulation}} \text{ X } 100$$

*2.2.7. DPA Release Study*

For *DPA* release, weighed polymeric nanoparticles were suspended in 2 ml phosphate buffer saline pH 7.4 was placed in sigma dialysis tubing. The tube containing dispersion of polymeric nanoparticles was then introduced into a 200 ml beaker containing 100 ml release media (phosphate buffer pH 7.4), which was stirred at 400 + 20 rpm using magnetic stirrer. Drug release was assessed by intermittently sampling the receptor media (5ml) at predetermined time intervals each time the 5 ml of fresh phosphate buffer saline pH 7.4 was replaced. The amount of drug release in the buffer solution was quantified by a UV spectrophotometer at lambda max[19].

## 3. Results and Discussions

3.1. *Chemistry*

*3.1.1. UV Studies*

UV-spectra of chitosan shows a sharp prominent peak at 190 nm and for 16-DPA, it shows the prominent band at 246 nm. In case of CHDPA product, it shows the peak at 259 nm. After conjugation reaction the shifted signal, indicating the formation of the new ketimine bond shown in Figure 1.

*3.1.2. Chitosan (CH)*

The FT-IR spectra of chitosan (CH) spectra shows characteristic band at 2920 $cm^{-1}$ to 3378 $cm^{-1}$ corresponds to N-H stretching with hydrogen bonded amino groups, 1726 $cm^{-1}$ peak is assigned to the C-O stretching (C=O in carboxylic acid), 1612 $cm^{-1}$ is due to amide I group (C-O stretching along with N-H deformation mode), 1560 $cm^{-1}$ peak is attributed to the $NH_2$ group due to N-H deformation, 1460 $cm^{-1}$ is assigned to the

symmetrical deformation of $CH_3$ and $CH_2$ group, 1425 $cm^{-1}$ peak is due to C-N axial deformation (amine group band), 1384 $cm^{-1}$ peak is due to COO- group in carboxylic acid salt, 1196 $cm^{-1}$ is assigned to the special broad peak of β (1- 4) glycosides band in polysaccharide unit, 1108 $cm^{-1}$ is attributed to the stretching vibration mode of the hydroxyl group, 1020 $cm^{-1}$ stretching vibration of C-O-C in glucose circle and 1060-1015 $cm^{-1}$ bands corresponds to CH-OH in cyclic compounds [20-21]. Band between at 590 to 770 due to O-C=O in carboxylic acid due to preparation of CS solution in acetate buffer solution. The absorption band at 1650 $cm^{-1}$ was attributed to the carbonyl of O=C-NHR of chitosan [22] and the absorption band at 1599 $cm^{-1}$ was assigned to the amino groups of chitosan with high deacetylation degrees. This signal shifted to 1528 $cm^{-1}$ after the conjugation reaction, indicating the formation of new amide bonds by acylation of amino groups of chitosan. A weak shoulder peak occurred at 1738 $cm^{-1}$ assigned to the carbonyl of ester bond of CS shown in Figure 2.

The $^1H$ NMR spectrum of chitosan shows the chemical shifts of the protons appears at 4.58 ppm for acetal proton (-CH) of the glucosamine, 3.01 ppm for -CH-$NH_2$, 3.75 ppm for -CH-OH, 3.59 ppm for -$CH_2$-OH and 1.94 ppm for acetamido protons (-NH-CO-$CH_3$).

The $^{13}C$ NMR spectra of chitosan shows : δ 98.3(C-1), 56.9(C-2), 70.9(C-3), 78.0(C-4), 75.7(C-5), 61.4(C-6).

3.1.3. *16- Dehydropregnenolone Acetate (16-DPA)*

$^1H$ NMR ($CDCl_3$): 1.0 (s, 3H, Me-19), 1.1 (s, 3H, Me-18), 1.3–2.2 (m, –CH and –$CH_2$), 2.0 (s, acetate proton), 2.3 (s. methyl ketone proton), 4.6 (m, 1H, C-3 Proton under acetate), 5.3 (m, 1H,C-6 olefinic proton), 6.7 (m,1H, 16-vinyl hydrogen); $^{13}C$ NMR

215 ($CDCl_3$): δ 31.5(C-1), 32.2(C-2), 76.6 (C-3), 46.0(C- 4), 144.4(C-5), 121.9(C-6), 30.1(C-
216 7), 31.5(C-8), 50.3.0(C-9), 38.1(C-10), 20.6(C-11), 27.7(C-12), 36.7(C-13), 36.8 (C-14),
217 31.5(C-15), 140.2(C-16), 144.4(C-17), 196.8(C-18), 19.2(C-19), 20.6(C-20), 21.4(C-21),
218 15.7 ($C–CH_3COO$), 170.5 (C–C=O); IR ($CHCl_3$) : 2933, 2851, 1732, 1666, 1435,
219 1245 $cm^{-1}$ [23].

220 3.1.4. *Chitosan – 16-dehydropregnanolone acetate ketimine Product*

221 IR spectra of Chitosan- dehydropregnanolone acetate ketimine Product shows
222 peaks at 3394 (br) $cm^{-1}$ for –OH stretching, 2929 and 2852 $cm^{-1}$ for C-H stretching, 1702
223 $cm^{-1}$ for C-O stretching of the acetyl group (amide II), 1649 $cm^{-1}$ corresponds to C=N
224 stretching (ketimine), N-H deformation ($NH_2$) peak is shifted to 1564 $cm^{-1}$, 1406 $cm^{-1}$ for
225 asymmetric C-H bending of $CH_2$ group and 1605 $cm^{-1}$ for CO-bridge stretching of
226 glucosamine residue.

227 The $^1H$ NMR spectrum revealed the signals at δ 3.2 for –NHCO- group, at 1.1 for
228 -NH- group, 4.6 (s-br, for H-1) of chitosan and 3.2–3.5 (s-sh, br, H-2, H-3, H-4, H-5 & 6)
229 for $CH_2OH$ the peak at 2.4 (s-sh), 1.0 (s, 3H, H-18), 1.3 (s, 3H, H-19), 7.2 (16-vinyl
230 hydrogen), 4.5 (s, 3H, methyl ketone).

231 In $^{13}C$ NMR of the product shows some new peaks at δ 49.8 (C-N-C), 176.5 (-
232 C=N-, ketimine) and 71.4 ($CH_2OH$) with other peaks of the steroid and chitosan part.

233 3.1.5. *SEM and TEM Analysis*

234 The general morphology of the product was investigated by SEM images. Figures
235 3a and b showed representative images of the nano rods with the image size 30-50 μm.
236 Moreover, the latter shows that the particles are aggregates consisting of much smaller
237 amorphous particles growing and has very small (300-500 nm) amorphous particles

comprise high surface. On the other hand, these particles are already amorphous, which makes them sufficiently stable in a system different from the starting one, they used to grow[7]. The presence of both, single isolated amorphous particles and complex aggregates, suggests that the growth process is promoted by two types of nanoparticles: (i) a single isolated bred released from the aggregates and (ii) complex aggregates comprising large number of single bred-nuclei.

The detailed microstructure of product CHDPA nanorods was further investigated by TEM images. The examination of the amorphous products shows that a great part of material is in the form of random aggregates [24] and the structure, self-aggregate behavior etc of CHDPA were shows in the TEM photographs in Figure 4a and b. The shapes of CHDPA nanoparticles observed were mostly spherical and cubical. The diameters of the nanoparticles were 300-500 nm.

Nevertheless, abundant intergrowth was observed in the products and the number of isolated well-shaped amorphous was limited. The most likely origin for the abundant intergrowth is the presence of nanoparticles, which are governing the growth in the system. The drawing in Figure 4a and b, supported by TEM images, represents the two types of particles. The domination of the aggregates in the product is in good agreement with the above suggestion. The mass of aggregated nanoparticles growing into amorphous is much higher than that of single bred nuclei. The low number of single isolated structure can be explained by either limited breeding or by the released bred nuclei staying in close proximity of parent aggregate and thus their development into amorphous results in complex aggregates. Therefore, the formation of nanoparticles with

narrow particle size distribution cannot be expected if the growth in the system is promoted by complex aggregates, even being with nanometric size.

3.2. *Biology*

The synthesized compound showed in good antifungal activity in general. The data and the experimental photographs are given in Table 1 and Figure 5(E1-E5).

The antifungal activity of the new modified chitosan (CHDPA) was studied against the fungus *Colletotrichum gleosporioides.* The inhibitory effects of the samples were tested in vitro on mycelia growth of *Colletotrichum gleosporioides* using Poisoned Food technique with the five concentrations of 100, 200, 300, 400 and 500 ppm. Data reveals that with increasing the concentration, inhibition percentage also increases.

*3.3. DPA Loading Capacity (LC), Encapsulation Efficiency (EE) and DPA Release study*

The synthesized products showed in good Drug loading capacity (LC) ie. 23.2% and encapsulation efficiency (EE) 20.9% respectively, which has been given in Table 2. And also showed the good release behavior described by the Figure 6.

## 4. Conclusion

In this contribution, we successfully utilized chitosan, a biocompatible polymer and steroid to synthesis chitosan-16-DPA nanoparticle linear aggregates. The chitosan employed herein, not only served as the reducing agent and stabilizer, but also led to the assembly of chitosan-16-DPA nanoparticles. TEM images and UV- spectra confirmed the existence of the nanoparticle linear aggregates in solution. One could obtain highly branched long chains and isolated short chains by adjusting the molar ratio of the chitosan repeat unit to 16-DPA. Moreover, the process of growth and assembly for the

chitosan-16-DPA nanoparticle was studied by SEM. This method provides a novel way to fabricate chitosan-16-DPA nanoparticle linear aggregates by virtue of its one-pot simplicity and chain-length tunability. From the analyzed result, compound was found to be the most promising antifungal activities against the fungus *Colletotrichum gleosporioides*. The drug loading capacity (LC) was found to be 23.2% and encapsulation efficiency (EE) was 20.9% respectively. The drug release study was investigated using UV spectrophotometer and shown in good result.

**Acknowledgement**

The authors thank the Director CSIR-North East Institute of Science & Technology, Jorhat, Assam for providing facilities and valuable advice and also gratefully acknowledge the financial assistance supported by DST, New Delhi and CSIR, New Delhi, INDIA.

## References


1. Liu, N.; Chen, X. G.; Park, H. J.; Liu, C. G.; Liu, C. S.; Meng, X. H. *Carbohydrate Polymer*. **2006**, 64, 60-65.

2. Chen, S. P.; Wu, G. Z.; Zeng, H. Y. *Carbohydrate Polymer*. **2005**, 60, 33-38.

3. Du, W. L.; Niu, S. S.; Xu, Y. L.; Xu, Z. R.; Fan, C. L. *Carbohydrate Polymers*. **2009**, 75, 385-389.

4. Knapczyk, J.; Krowczynski, L.; Krzck, J.; Brzeski, M.; Nirnberg, E.; Schenk, D.; Struszcyk, H. *Requirements of chitosan forpharmaceutical and biomedical applications*. In: Skak-Braek G, Anthonsen T, Sandford P (eds) *Chitin and chitosan: sources,chemistry, biochemistry, physical properties and applications*. Elsevier, London, pp 657–663, 1989.

5. Prabaharan, M.; Mano, J. F. *Macromol. Biosci.* **2006**, 6, 991-1008.

6. Prabaharan, M.; Rodriguez-Perez, M. A.; de Saja, J. A.; Mano, J. F. *J. Biomed. Mater. Res. Part B: Appl. Biomater.* **2007**, 81, 427-434.

7. Gong, J.; Hu, X.; Wong, K. W.; Zheng, Z.; Yang, L.; Lau, W. M.; Du, R. *Adv. Mater.* **2008**, 20, 2111-2115.

8. Suh, J-K. F.; Matthew, H. W. T. *Biomaterials*. **2000**, 21, 2589-2598.

9. Jia, X.; Chen, X.; Xu, Y.; Han, X.; Xu, Z. *Carbohydrate Polymers.* **2009**, 78, 323-329.

10. Kumar, M. N. V. R.; Muzzarelli, R. A. A.; Muzzarelli, C.; Sahiwa, H.; Domb, A. J. *Chemical Reviews.* **2004**, 104, 6017-6084.

11. Mao, H. Q.; Roy, K.; Troung-Le, V. L.; Janes, K. A.; Lin, K. Y.; Wang, Y. *Journal of Control Release.* **2001**, 70, 399-421.

12. Du, W. L.; Xu, Z. R.; Han, X. Y.; Xu, Y. L.; Miao, Z. G. *Journal of Hazardous Material*. **2008**, 153, 152-156.

13. Qi, L.; Xu, Z.; Chen, M. *European Journal of Cancer.* **2007**, 43(1), 184-193.

14. Chien, P. J.; Seu, F.; Yang, F. H. *Journal of Food Engineering*. **2007**, 78, 225-229.

15. Xu, Y.; Du, Y. *International Journal of Pharmaceutics*. **2003**, 250, 215-226.

16. Yang, W. Z.; Zhang, Q. Q.; Chen, H. L.; Li, X. M.; Jiang, Q.; Chen, M. M.; Gao, F. P.; Zhang, H. Z.; Yi P.; Xiaohong W. 7th APCMBE 2008 Proceedings, 19, 13.

17. Grover, R. K.; Moore, J. D. *Sclerotinia fructicola* and *S. Laxa. Phytopathology*. **1962**, 52, 876-880.

18. Ogbebor, O. N.; Adekunle, A. T. *African Journal of General Agriculture.* **2008**, 4(1), 19-26.

19. Dhana lekshmi, U. M.; Poovi, G.; Narra, K.; Neelakanta Reddy, P. *International Journal of Pharmaceutics,* **2010**, 396, 194-203.

20. Biemann, K. *Spectral Data for Structure Determination of Organic Compounds*, Second Edition, Springer-Verlag, New York, 1983.

21. Tian, F.; Liu, Y.; Hu, K.; Zhao, B. *J. Mate. Sci*. **2003**, 38, 4709-4712.

22. Osman, Z.; Arof, A. K. *Electrochimica Acta*. **2003**, 48, 993-999.

23. Chowdhury, P. K.; Borah, J. M. Goswami, P.; Das, A. M. *Steroids*. **2011**, 76, 497-501.

24. Leng, B.; Chen, X.; Shao, Z. Z.; Ming, W. *Small*. **2008**, 4, 755-758.

**List of Table, Schemes, Figures have been given below.**

**Table 1 : The Inhibitory effects of the samples on mycelia growth of C and 7 days after inoculation (percent inhibition).**

**Table 2 : Effect of percent of drug loading capacity (LC) and encapsulation Efficiency (EE) of Chitosan-16DPA**

**Scheme 1 : Schematic representation of reaction mechanism for Chitosan-16DPA**

**Figure 1 : UV-vis spectra (A) Chitosan and (B) (a) 16-DPA (b) Chitosan-16DPA**

**Figure 2 : FT-IR spectra (A) Chitosan and (B) (a) 16-DPA (b) Chitosan-16DPA**

**Figure 3 : SEM photographs of Chitosan-16DPA (a,b)**

**Figure 4 : TEM Photographs of Chitosan-16DPA (a,b)**

**Figure 5 : Antifungal activity : C= Control E1 – E5 = Experimental concentrations of 100, 200, 300, 400 & 500 ppm.**

**Figure 6 : In vitro study of Chitosan-16DPA**

**Table 1 : The Inhibitory effects of the samples on mycelia growth of C and 7 days after inoculation (percent inhibition).**

| Samples | Concentrations (ppm) | | | | |
|---|---|---|---|---|---|
| | 100<br>Mean ± SD | 200<br>Mean ± SD | 300<br>Mean ± SD | 400<br>Mean ± SD | 500<br>Mean ± SD |
| CHDPA | 74.7 ± 0.98 | 75.8 ± 0.51 | 78.4 ± 1.57 | 81.0 ± 0.65 | 83.6 ± 0.86 |
| Control | Full growth of the fungus | | | | |

**Table 2 : Effect of percent of drug loading capacity (LC) and encapsulation efficiency (EE) of Chitosan-16DPA.**

| Samples | % | |
|---|---|---|
| | Drug loading capacity (LC) | Encapsulation efficiency (EE) |
| CHDPA | 23.2 | 20.9 |

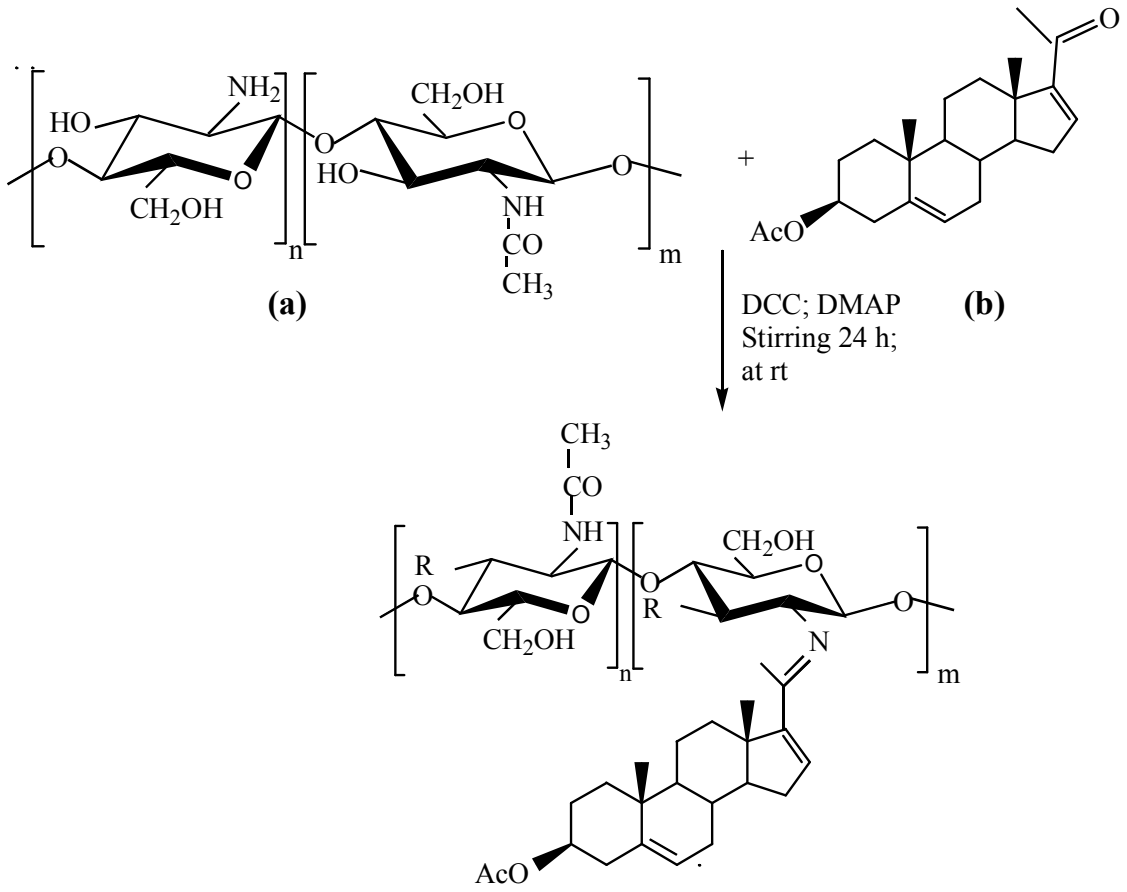


415

416 **Scheme 1 : Schematic representation of reaction mechanism for Chitosan-16-DPA.**

417

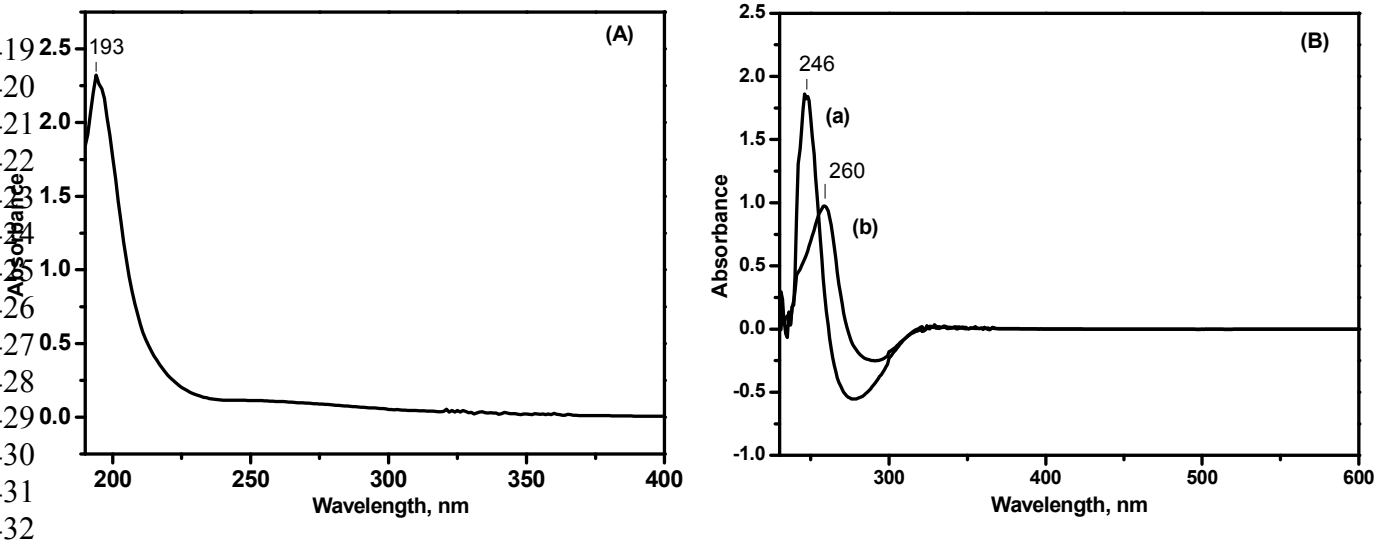


**Figure 1 : UV-vis spectra (A) Chitosan and (B) (a) 16-DPA (b) Chitosan-16-DPA.**

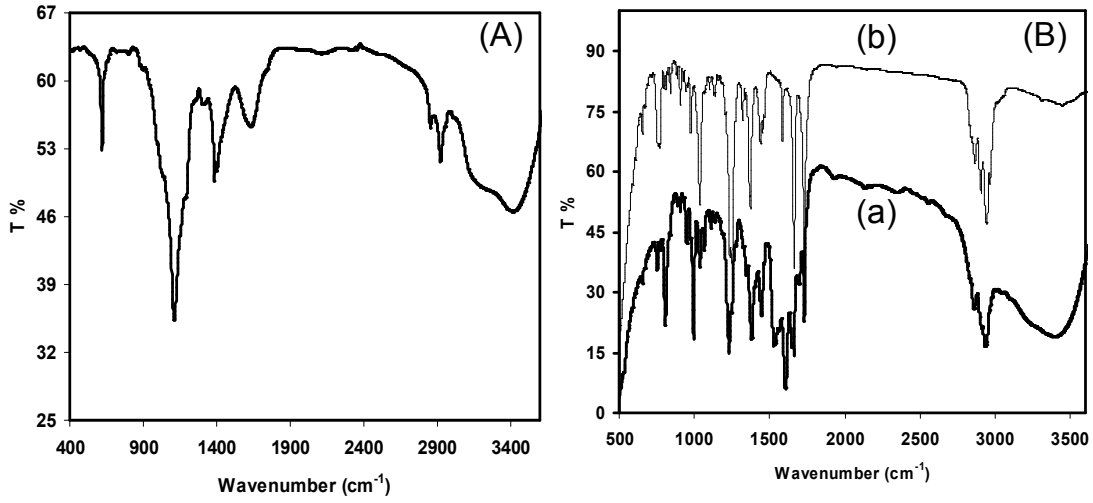


**Figure 2 : FT-IR spectra (A) Chitosan and (B) (a) 16-DPA (b) Chitosan-16-DPA.**

440

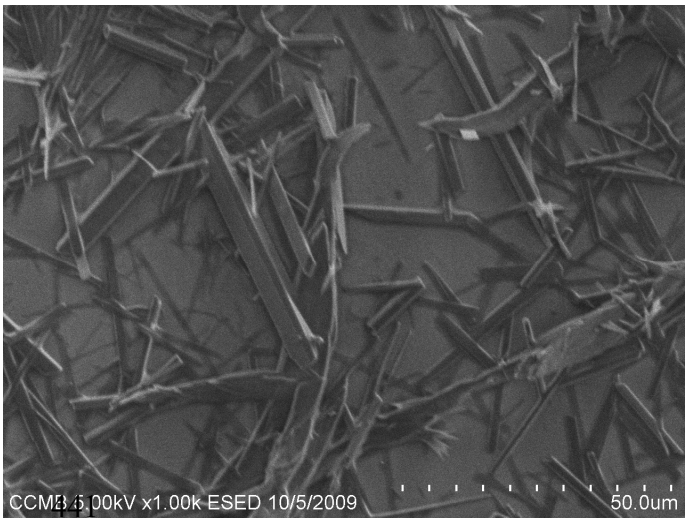


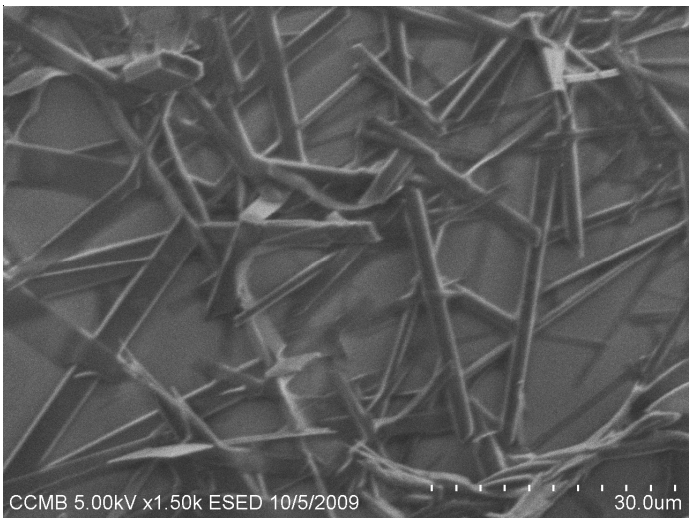


442 **(a)** **(b)**

443 **Figure 3 : SEM Photographs of Chitosan-16DPA.**

444

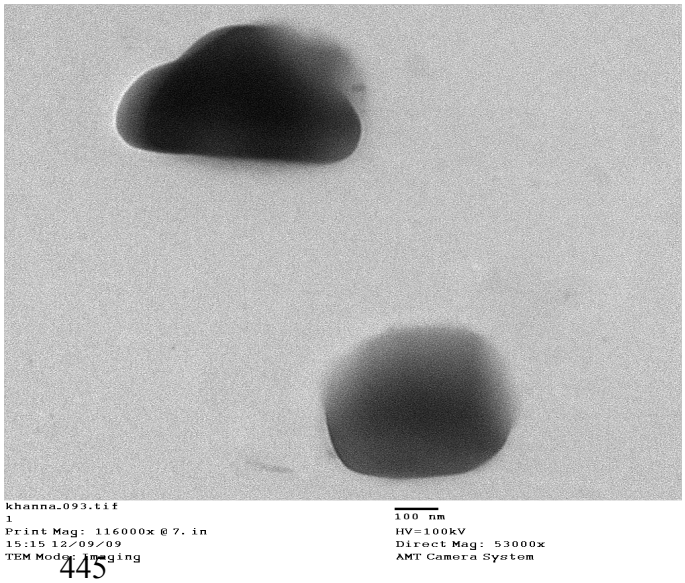


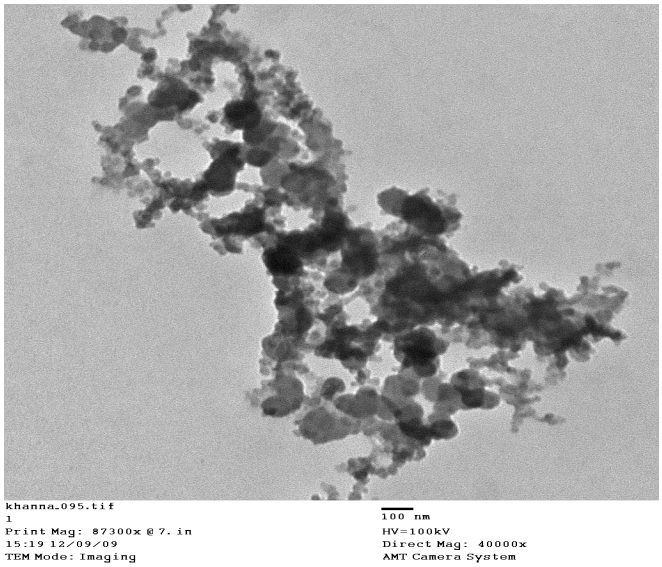


445

446 **(a)** **(b)**

447 **Figure 4 : TEM photographs of Chitosan-16DPA.**

448

449

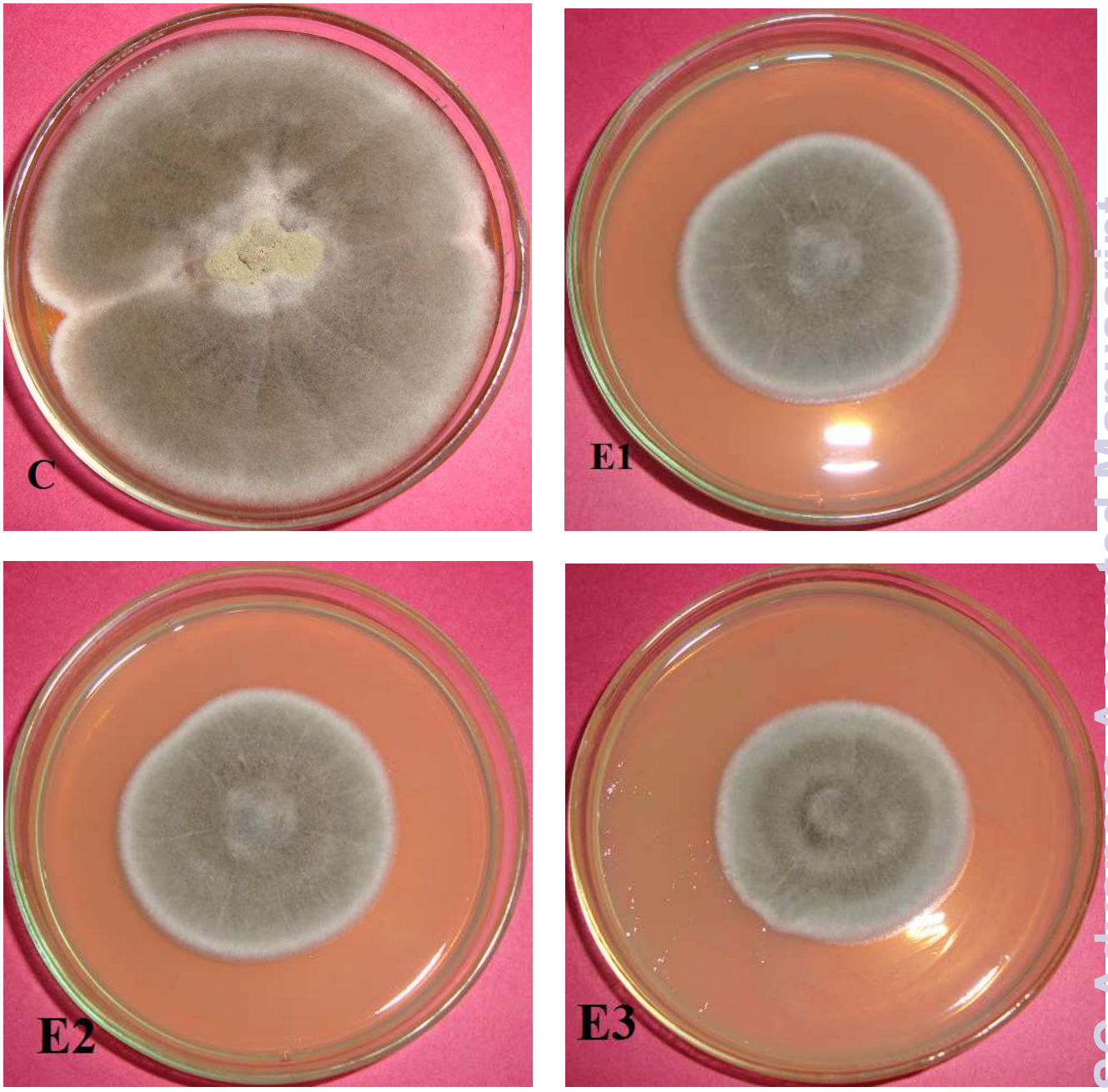


450
451
452
453

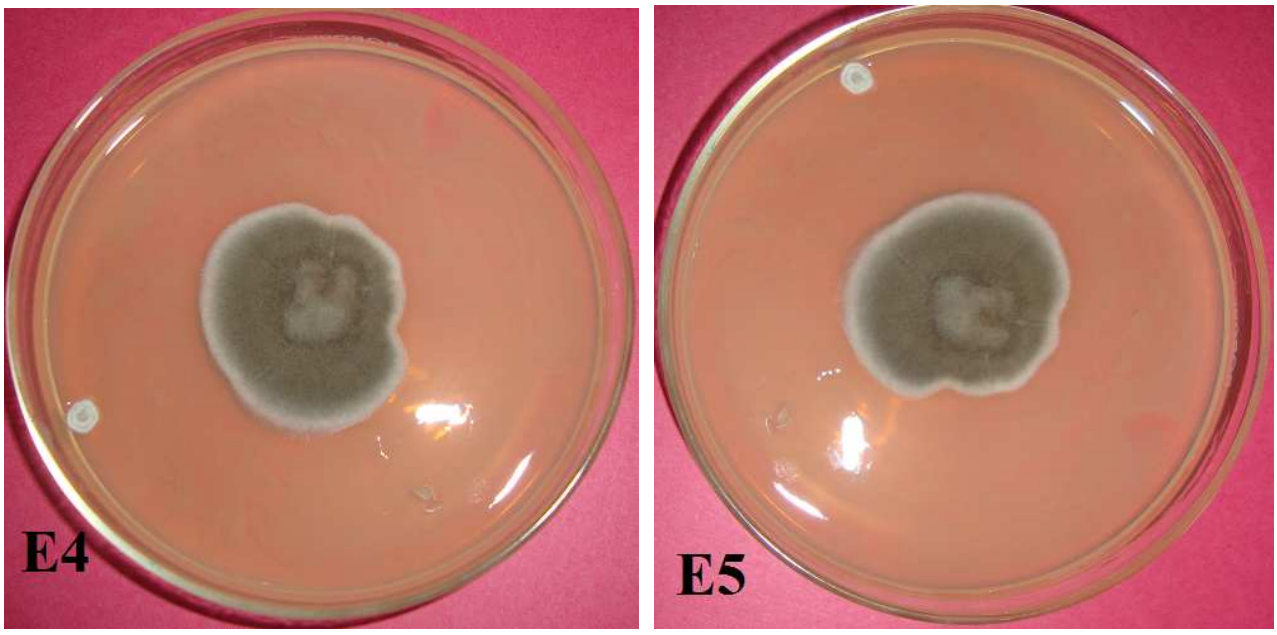


**Figure 5 : Antifungal activity : C= Control E1 – E5 = Experimental concentrations of 100, 200, 300, 400 & 500 ppm.**

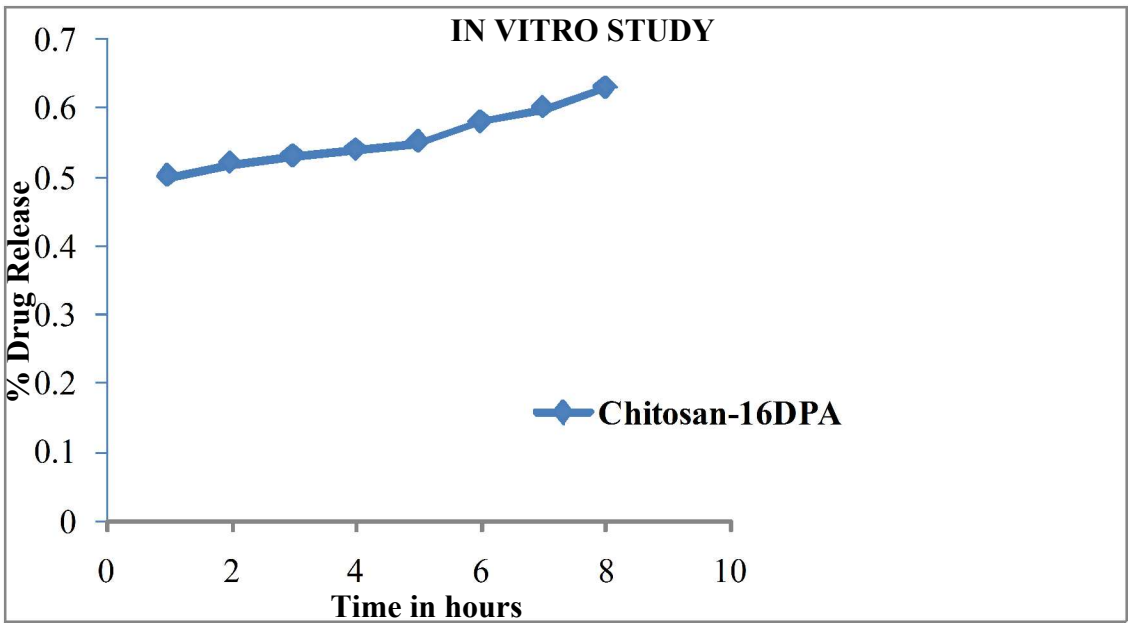


**Figure 6 : In vitro study of Chitosan-16DPA.**